Int'l Journal of Advances in Chemical Engg., & Biological Sciences (IJACEBS) Vol. 4, Issue 1 (2017) ISSN 2349-1507 EISSN 2349-1515

Kinetics and Thermodynamics of Methyl Orange Uptake from Model Effluent by Watermelon Shells and Neem Leaves

Sadiq Sani[1] and Haruna Abdullahi[2]

***Abstract*—**The adsorption kinetics and thermodynamics of methyl orange dye removal from model dyeing effluent by cheap watermelon (Citrullus lanatus) shells (WSA) and neem (Azadirachta indica) leaves (NLA) adsorbents were investigated. Kinetic parameters of pseudo-first order (PS-1), pseudo-second order (PS-2), intraparticle diffusion (IP-D) and Elovich's (EL-V) models for the dye adsorption onto the adsorbents were determined. Linear coefficients of determination (R^2) for all the models were in the range 0.0411-0.9224 for WSA and 0.4241-0.9979 for NLA. The goodness-of-fit of the models for the dye uptake onto both adsorbents was in the order PS-2 > PS-1 > IP-D > EL-V with the PS-2 model having the best and EL-V model having the least fitting of the experimental data in each case. Adsorption rate constants for the models also followed similar pattern with the best rate in PS-2 model (k_2 for WSA: 17.2726 $g.mg^{-1}.min^{-1}$ and k_2 for NLA: 55.8756 $g.mg^{-1}.min^{-1}$) and the least in EL-V model (α for WSA: 5.88×10^{-23} $g.mg^{-1}.min^{-1}$ and α for NLA: 2.87×10^{-11} $g.mg^{-1}.min^{-1}$). Error analyses and χ^2-test of the data confirmed NLA to be a better adsorbent than WSA but both adsorbents are potentially effective for the dye removal from the effluent.

***Keywords*—**methyl orange, watermelon shell, neem leaves, kinetic models, thermodynamics.

I. INTRODUCTION

WATER pollution is a global phenomenon posing significant challenges to the effective conservation of natural water resources such as the oceans, seas and rivers for sustainable development. Uncontrolled anthropogenic industrialization, urbanization, agriculture, release of hazardous wastes and rapid population growth are believed to be its main sources [1][2]. A wide range of pollutants, harmful to both humans and the environment, are found in effluents from such sources [3]. One such group of pollutants are synthetic organic dyes released as untreated aqueous dyeing effluents into adjacent water bodies through dye manufacturing and processing operations by cosmetics, food, leather, paper and pulp, plastic and rubber, printing and textiles industries. The presence of dyes in aqueous dyeing effluent has significant adverse effects in the environment due to their high toxicity to humans and aquatic biota; they have excessively visible colour resistant to degradation by light, chemical action and microorganisms; and inhibit photosynthesis in aquatic plants by shielding light and oxygen from penetrating to the bottom of the water body [1][5-7]. Dyes have also been ascertained to cause cancer, jaundice, tumors, skin irritation, allergies, heart defects and mutations in humans [1][7][8]. To sustainably overcome global water scarcity, dye-polluted water has to be reclaimed using an effective treatment method, reused and recycled.

A number of physical, chemical and biochemical techniques have been previously employed for removal of dye molecules from untreated effluents. A large number of these techniques were proved ineffective due to production of large amounts of secondary pollutant sludge, needed highly trained personnel and have high cost of maintenance. One effective and attractive method in the treatment of such effluents is the adsorption process using natural and synthetic low cost adsorbents such as fly ashes and zeolites [9], Kaolin [10], kola nut shell activated carbons [11], chitosan beads [12], rice husk and egussi peelings [13], neem and mango barks [14] natural and modified orange peel [15] and neem leaf [16]. The present study is aimed at conducting laboratory scale batch adsorption experiments to evaluate select kinetics models and thermodynamics parameters of methyl orange dye removal from synthetic aqueous dyeing effluent onto watermelon shell (WSA) and neem leaves (NLA) as locally available low-cost adsorbents from Katsina, Nigeria. The influence of the dye pH, contact time and temperature for the two dye-adsorbent combinations were also investigated.

II. MATERIALS AND METHODS

A. Preparation of adsorbents and Chemicals

An analytical grade methyl orange dye (*p*-dimethylamino-azobenzenesulphonic acid sodium salt) used in this work was procured from BDH Laboratory Supplies Poole, England and was used as received without further purification. It is a mono-azo dye with the structure shown in Figure 1. A stock solution containing 1000 mg/L of the dye was prepared by accurately weighing 1.0 g of the dye solute into 1000-mL volumetric flask and dissolution to the graduated mark with de-ionized water [17]. All desired concentrations of calibrations and working standards were prepared by serial dilution for subsequent experiments. Analytical grade NaOH and HCl were supplied from Merk Company. Adsorbents employed in this research work were derived from the fresh samples of watermelon (*Citrullus lanatus*) shells and neem-tree

---

[1,2]Department of Applied Chemistry, Federal University Dutsinma, P.M.B. 5001, Dutsin-Ma, Katsina State, Nigeria.

https://doi.org/10.15242/IJACEBS.ER0117011

(*Azadirachta indica*) leaves as waste adsorbents. While the watermelon shells were collected from local fruit sellers, neem leaves were collected from matured branches of neem-trees both in Katsina Metropolis.

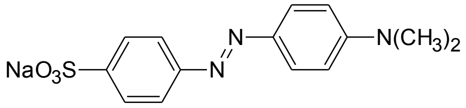

Fig. 1: Structure of methyl orange dye

The watermelon shells collected were prepared in accordance with the procedure in the literature [20][21]. First, the shells were copiously washed with tap-water followed by distilled water to remove any impurities such as debris or dust particles on their surfaces. The shells were sliced into small cubes (around 1 to 2 mm^3), dried by exposure to sunlight for 96 hours spread on trays and oven-dried at 333 K for 48 hours. Dried shells were pulverized, sieved to ≤75 μm mesh particle sizes and stored in desiccators as watermelon shells-based adsorbent (WSA) for subsequent use. Except for the slicing step, the same procedure was repeated on neem leaves and preserved in desiccators as neem leaves-based adsorbent (NLA) for further experiments.

B. Batch Adsorption Studies

A modified static batch adsorption procedure based on Gumus (2016) and Ciobanu et al. (2016) was employed to study dye adsorption onto the powdered adsorbents (WSA and NLA) by transferring 50 mL aliquots of 300 mg/L concentration of freshly prepared methyl orange at a fixed pH into a 250-mL conical flask containing 500 mg dosage of the adsorbent of ≤75 μm mesh particle sizes. The mixture was then placed into a thermostatic shaker set at room temperature (298.15 K), constant agitation speed of 150 rpm and for a predetermined contact time. Maintaining all conditions, experiments to investigate the effect of the dye initial pH on adsorption capacity of each adsorbent were performed within the pH range of (2, 4, 6, 7, 8, 10 and 12) at a specific constant time of 60 minutes. Analysis of the influence of contact time was performed within the range (5, 10, 15, 30, 45, 60, 90 and 240 minutes) under the same conditions but at equilibrium pH of dye adsorption attained on each of the two adsorbents. Under identical conditions but at equilibrium adsorption pH and equilibrium contact time for dye adsorption onto each adsorbent, the effect of temperature change within the range (303.15, 313.15, 323.15 and 333.15 K) on dye adsorption onto each adsorbent was studied. At equilibrium or predetermined time, portions of the dye supernatant solution were withdrawn and filtered through a Whatman filter paper No. 4, discarding the first few volume of the filtrate. Estimation of the residual dye concentrations in the filtrates was performed by transforming their corresponding absorbance values recorded at maximum absorption wavelength (λ_{max}) of 464 nm on a UV-visible spectrophotometer (T60 PG Instruments) [20][21]. The amount of dye adsorbed at equilibrium and at time t were determined using Equations 1 and 2 respectively.

$$Q_e = \frac{(C_O - C_e)}{M}.\mathrm{V} \tag{1}$$

$$Q_t = \frac{(C_O - C_t)}{M}.\mathrm{V} \tag{2}$$

where C_O is the initial dye concentration (mg/L), C_e is the equilibrium concentration (mg/L), C_t is the final dye concentration (mg/L) at time t, Q_e is the amount of dye adsorbed at equilibrium (mg/g), Q_t is the amount of dye adsorbed at equilibrium time (mg/g), M is the mass of the adsorbent (g), V is the volume of dye solution (mL)..

C. Kinetics and Thermodynamics Studies

To determine whether the probable rate-determining step of the MO dye adsorption onto the adsorbents (WSA and NLA) involved mass transport, pore diffusion or chemical reactions mechanisms, kinetic models such as the pseudo-first order rate, pseudo-second order rate, intra-particle diffusion rate and Elovich's rate equations were employed on the data from batch experiments. The linear transformations of these models are represented by Equations (3), (4), (5) and (6) respectively [3][11].

$$\ln(Q_e - Q_t) = \ln Q_e - k_1 t \tag{3}$$

$$\frac{\mathrm{t}}{Q_t} = \frac{t}{k_2 Q_e^2} + \frac{\mathrm{t}}{Q_e} \tag{4}$$

$$Q_t = k_t t^{1/2} + I \tag{5}$$

$$Q_t = \frac{1}{\beta}\ln(\alpha\beta) + \frac{1}{\beta}\ln(t) \tag{6}$$

where k_1 is the pseudo-first order rate constant (min^{-1}), k_2 is the pseudo-second order rate constant ($mg.g^{-1}.min^{-1}$), t is the contact time (min), I is the initial adsorption capacity at time $t = 0$, α is a constant equivalent to initial sorption rate ($mg.g^{-1}.min^{-1}$) and β is a constant related to the extent of surface coverage and activation energy of chemisorptions [3].

D. Thermodynamics Studies

To assess the thermodynamics of the process, equilibrium thermodynamic parameters including entropy change (ΔS^O), enthalpy change (ΔH^O) and Gibb's free energy change (ΔG^O) were determined at various temperatures using Van't Hoff plots (Equation 11) of lnK_o against $1/T$, as well as Equations (9) and (10).

$$\Delta G^O = -RT\ln K_O \tag{7}$$

$$\Delta G^O = \Delta H^O - T\Delta S^O \tag{8}$$

E. $$\ln K_O = \frac{\Delta S^O}{R} - \frac{\Delta H^O}{RT} \tag{9}$$

where K_O is the distribution coefficient, R is the ideal gas constant (8.314 $J.mol^{-1}.K^{-1}$) and T is the absolute temperature (K).

F. Error analysis of kinetics data

Linearization of the kinetic models incorporates into the data an inherent bias that necessitates the employment of non-linear regression tests based on the evaluation of four selected error functions as criteria for the fitting quality of the models which include root mean square error (RMSE), chi-square test (χ^2-test), sum of the absolute errors (SAE) and average relative error (ARE) [1]. Numerous investigators and researcher have employed the RMSE (Equation (10)) in testing the adequacy and accuracy of fitting the experimental data with the kinetics models.

$$RMSE = \sqrt{\frac{1}{N-2}\sum_{i=1}^{N}(Q_{ei,\exp} - Q_{e,cal})^2} \tag{10}$$

where $Q_{ei,exp}$ is the experimental sorption capacity from the batch experiment i, $Q_{ei,cal}$ is the sorption capacity estimated from the sorption model and N is the number of observations in the batch adsorption experiment. The χ^2-test statistic (Equation (11)) has some similarity with the RMSE. It is fundamentally the sum of the squared differences between the experimental sorption capacity and the sorption capacity calculated from models, with each squared difference divided by the sorption capacity calculated from models [1].

$$\chi^2 = \sum_{i=1}^{N}\frac{(Q_{ei,\exp} - Q_{e,cal})^2}{Q_{e,cal}} \tag{11}$$

Sum of the absolute errors (SAE) is given by Equation (12). The kinetic parameters determined by this method provide a better fit as the magnitude of the errors increase, biasing the fit towards the data with high concentration [1].

$$SAE = \sum_{i=1}^{N}\left|Q_{ei,\exp} - Q_{e,cal}\right| \tag{12}$$

The average relative error (ARE) is defined by Equation (13). This error function is purposely used to minimise fractional error distribution across the entire concentration range [1].

$$ARE = \frac{100}{N}\sum_{i=1}^{N}\left|\frac{Q_{ei,\exp} - Q_{e,cal}}{Q_{ei,\exp}}\right| \tag{13}$$

III. RESULTS AND DISCUSSION

A. *Effect of initial pH of dye*

The influence of change in pH of the aqueous dye solution on the amount of the dye ions removed (mg.g^{-1}) onto the adsorbents (WSA or NLA) was studied by the addition of few drops of either 0.1 M NaOH (aq) or 0.1 M HCl (aq) to the dye solution in order to appropriately adjust the pH from 2.0 to 12.0. As shown in Figure 2, the amount of the anionic methyl orange (MO) dye removed from the model effluent by WSA was observed to increase rapidly from 22.40 mg.g^{-1} to its maximum value of 24.88 mg.g^{-1} when the solution pH was increased from 2.0 to 4.0. The adsorption capacity decreased from its peak value until it reached a steady equilibrium value around 23.18 mg.g^{-1} that did not change significantly with pH at pH of 7.0 it further decrease significantly to 22.62 mg.g^{-1} at pH of 12. Similarly, the removal of the anionic dye by NLA was found to increase rapidly from 23.96 mg/g to its maximum value of 26.38 mg.g^{-1} when the initial pH of the dye was increased from 2.0 to 4.0. Further decrease in the adsorption capacity of the adsorbent from its peak value to a steady equilibrium value of 24.73 mg.g^{-1} at pH of 7.0 was observed. The increase in adsorption capacity of the adsorbents under acidic condition (at low pH) was due to the higher degree of protonation of its surface active sites, which brought about increased adsorbate-adsorbent electrostatic attraction, enhanced diffusion of dye adsorbates towards the adsorbent surface pores and increased dye adsorption onto the adsorbent. At higher pH values, the degree of protonation of the adsorbents' surface sites decreased leading to decreased electrostatic attraction, diffusion of dye adsorbates onto the surface pores and dye adsorption onto the adsorbents [11].

B. *Contact Time Study*

Studies on the influence of change in contact time t (min) on the amount of methyl orange dye ions removed Q_t (mg.g^{-1}) from the dye effluent by the adsorbents (WSA or NLA) were carried out. Figure 3 illustrates this relationship graphically. Initially, the dye removal capacity of both adsorbents increased rapidly with increase in contact time until it reaches a peak value. It then approaches relatively constant value by decreasing slowly before finally attaining an equilibrium value at an equilibrium time.

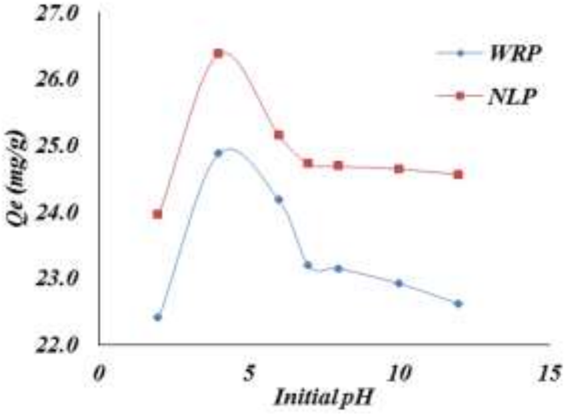

Fig. 2: Effect of initial pH on MO dye adsorption onto WSA and NLA adsorbents

Specifically, dye removal by WSA rose to 14.05 mg/g at 10 minutes until reaching a maximum (24.86 mg.g^{-1}) at 45 minutes and attaining equilibrium value (21.83 mg.g^{-1}) at 120 minutes. Similarly, dye removed by NLA rose to 20.83 mg.g^{-1} at 5 minutes before reaching a maximum (29.92 mg.g^{-1}) at 10 minutes and attaining equilibrium value (28.89 mg.g^{-1}) at 45 minutes. While 120 minutes was the optimum contact times of saturating WSA with the dye, 45 minutes was was the optimum For saturating NLA with the same dye.

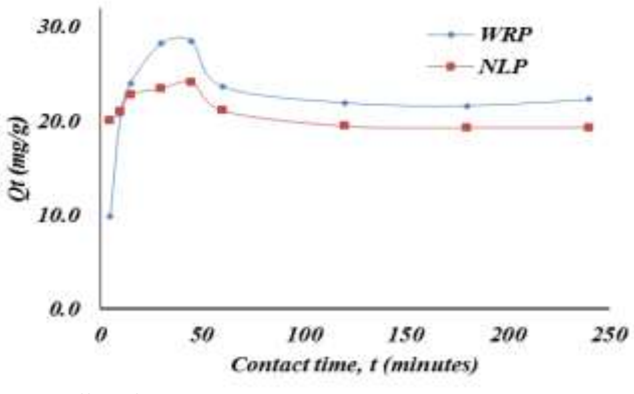

Fig. 3: Effect of contact time on MO dye adsorption onto WSA and NLA adsorbents

C. *Effect of Adsorption Temperature*

Adsorption temperature is a significant parameter that affects organic dye removal from aqueous effluents. Investigations of its impact on the adsorption capacity of the adsorbents were conducted at four different temperatures within the range of 303.15 K to 333.15 K, at constant initial dye concentration (300 mg/L), equilibrium contact time (120 min), adsorbent dose (0.5 g), particle size (≤75 µm) and optimum initial pH (7.0). As shown in Figure 4, the adsorption capacity of WSA was observed to increase from 24.80 $mg.g^{-1}$ to 25.59 $mg.g^{-1}$ while that of NLA increased from 27.88 $mg.g^{-1}$ to 28.69 $mg.g^{-1}$ when the temperature was increased from 303.15 K to 333.15 K respectively. Generally, rise in adsorption temperature has been known to cause increase in the diffusion rate of the adsorbate molecules across the external boundary layer between the adsorbent and the effluent solution as well as in the internal pores of the adsorbent particle, resulting in the solution viscosity lowering [22]. It is evident from the figure that the adsorption process was endothermic and the increased adsorption capacity of the adsorbents for the dye as the adsorption temperature increased was due to the corresponding increase in the rate of diffusion of the dye molecules into the adsorbent pores and decrease in the viscosity of the aqueous dyeing effluent [23].

D. *Adsorption Kinetics Studies*

Parameters of the various adsorption kinetics models, obtained at constant initial dye concentration of 300 mg/L, contact time range of 10-240 min, adsorbent dose of 0.5 g, adsorbent particle size of ≤75 µm and initial pH of 7.0 for WSA and 8 for NLA, are summarized in Table I. In all instances and for both adsorbents, the linear coefficient of determination (R^2) is higher for the pseudo-second-order than for other tested models. The values of the coefficient for Pseudo-first Order (PS-1), Pseudo-second Order (PS-2), Intraparticle Diffusion (IP-D) and Elovich's kinetic (EL-V) models were 0.5719, 0.9979, 0.5474 and 0.4241 for MO adsorption onto NLA and 0.1675, 0.9224, 0.1152 and 0.0411 for MO removal onto WSA respectively.

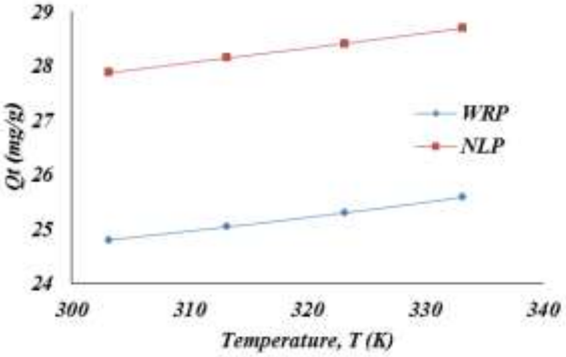

Fig. 4: Effect of temperature on MO dye adsorption onto WSA and NLA adsorbents

TABLE I: Parameters of Adsorption Kinetics Models

Kinetics Model	Parameter	WSA	NLA
Pseudo-first Order	$Q_{e,cal}$ ($mg.g^{-1}$)	14.7863	17.1209
	$Q_{e,exp}$ ($mg.g^{-1}$)	21.9123	19.4363
	k_1 (min^{-1})	0.0003	0.0003
	R^2	0.1675	0.5719
	RMSE	73.4225	130.8082
	χ^2-test	34.76 ($p = 2.96\times10^{-5}$)	53.48 ($p = 8.70\times10^{-9}$)
	SAE	736.1557	1006.9637
	ARE	117.7795	144.4337
Pseudo-second Order	$Q_{e,cal}$ ($mg.g^{-1}$)	3.3693	6.6890
	h ($g.mg^{-1}.min^{-1}$)	196.1	2500
	k_2 ($g.mg^{-1}.min^{-1}$)	17.2726	55.8756
	R^2	0.9224	0.9979
	RMSE	24.8921	0.6087
	χ^2-test	51.72 ($p = 1.91\times10^{-8}$)	0.64 ($p = 0.9997$)
	SAE	407.7360	52.8103
	ARE	51.0455	7.0768
Intraparticle Diffusion Model	k_{id} ($g.mg^{-1}.min^{-1}$)	0.0744	0.1063
	I	8.5656	7.9855
	R^2	0.1152	0.5474
Elovich's rate Model	β (g/mg)	5.7241	2.7196
	α ($g.mg^{-1}.min^{-1}$)	5.88×10^{-23}	2.87×10^{-11}
	R^2	0.0411	0.4241

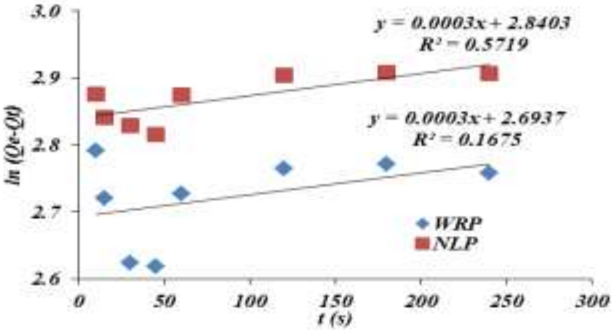

Fig. 5: Pseudo–first order kinetics for sorption of MO unto WSA and NLA

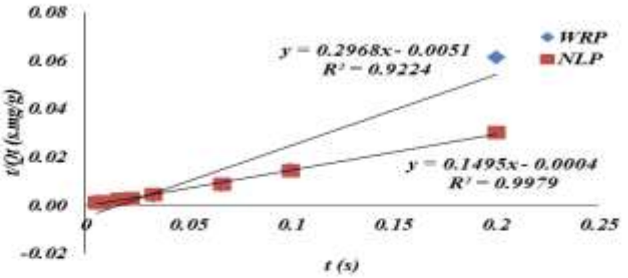

Fig. 6: Pseudo–second order kinetics for sorption of MO unto WSA and NLA

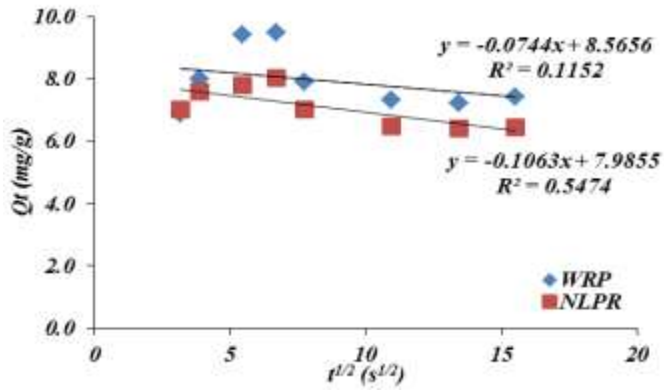

Fig. 7: Intraparticle diffusion kinetics for sorption of MO unto WSA and NLA

As shown in Figures 5, 6, 7 and 8, the value of the coefficient revealed that the fitting of the kinetic data for MO removal onto both adsorbents was in the order PS-2 > PS-1 > IP-D > EL-V with PS-2 giving the best fittings for the experimental data on both adsorbents. This indicated that the removal of the methyl orange dye molecules onto the adsorbents might have followed pseudo-second-order model apparently controlled by the chemisorption process [24]. Accordingly, the pseudo-second-order model could explain the dye uptake onto both plant-based adsorbents by adsorption process. The results suggested that the adsorption of the anionic MO dye onto the watermelon shell and neem leaves adsorbents might have occurred via chemisorption mechanism [24]. Similar observations were reported by [25].

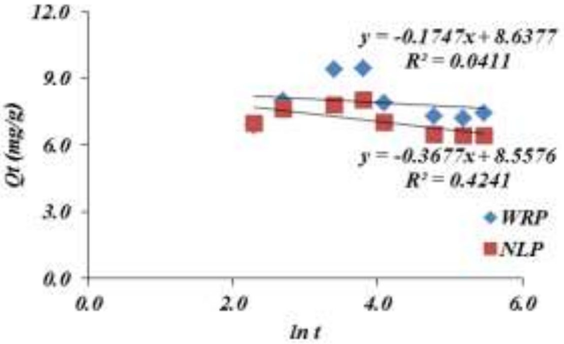

Fig. 8: Elovich's kinetics for sorption of MO unto WSA and NLA

E. *Thermodynamics Study*

Thermodynamics plots and thermodynamic parameters for the adsorptive removal of MO dye onto WSA and NLA are enumerated in Figure 9 and Table II respectively. The negative values of standard Gibb's free energy change obtained from the results suggested that adsorption processes for the dye removal onto both adsorbents were spontaneous but with higher spontaneity onto WSA than onto NLA (Awala and El Jamal, 2011). As the temperature was being elevated, the absolute Gibbs free energy change increased indicating that the reaction occurred with more ease at higher temperatures [25]. The value of ΔH^O and ΔS^O were found to be 5.4434 kJ.mol^{-1} and 0.0309 kJ.mol^{-1} for adsorption onto WSA and 4.3822 kJ/mol and 0.0248 kJ.mol^{-1} for adsorption onto NLA respectively. Positive values of ΔH^O for adsorption onto each of the two adsorbents further confirmed the process to be endothermic in nature [26]. The positive value of ΔH^O and ΔS^O for both adsorbents revealed the adsorption reaction to be favourable for both enthalpy change and entropy change. The positive value of ΔS^O denoted increase in randomness at the solid-solution interface, that enhanced effective encounters between the sorbent particles and sorbate dye molecules which led to higher probability of favourable adsorption [26]. Similar observations were made in the literature [26] during the adsorptive removal of copper metal ions from its aqueous solution using activated carbons.

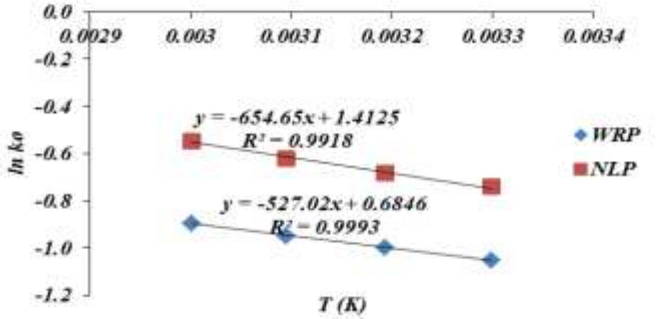

Fig. 9: Thermodynamic plots for adsorption of MO unto WSA and NLA.

TABLE II: Thermodynamic parameters for MO adsorption onto WSA and NLA

Adsorbent	T (K)	Thermodynamic Parameters		
		ΔG (kJ/mol)	*ΔH (kJ/mol)*	*ΔS (kJ/mol)*
WSA	303.15	-3.9210	5.4434	0.0309
	313.15	-4.2299		
	323.15	-4.5388		
	333.15	-4.8477		
NLA	303.15	-3.1476	4.3822	0.0248
	313.15	-3.3960		
	323.15	-3.6444		
	333.15	-3.8928		

IV. CONCLUSION

This study indicated that the experimental data on the kinetics of methyl orange dye removal from its synthetic aqueous effluent onto the WSA and NLA adsorbents was described by pseudo-second order model to a very large extent and to some little extents by pseudo-first order, intraparticle diffusion as well as Elovich's models. Whereas the pseudo-second order adsorption kinetics equation was the best model that described the experimental data of the dye removal onto the adsorbents, the Elovich's rate equation was least followed by the data. Values of the thermodynamics parameters calculated have shown the process to be endothermic for both adsorbents. Equilibrium sorption capacities of the two adsorbents were dependent on adsorption temperature, effluent pH (7-8) and contact time (10-240 min). Error analyses and χ^2-test probability showed NLA to be a better adsorbent than watermelon shells for methyl orange dye uptake from the effluent. Therefore, neem leaves and watermelon shell are potentially efficient sorbents for methyl orange dye removal from dyeing effluents due to their availability in large abundance as nuisance waste materials in the environment.

REFERENCES

[1] N.Ali, A. Hameed and S. Ahmed, "Physicochemical characterization and bioremediation perspective of textile effluent, dyes and metals by indigenous bacteria," *Journal of Hazardous Materials*, vol. 164, pp. 322–328, 2009. https://doi.org/10.1016/j.jhazmat.2008.08.006

[2] E. Alver and A.Ü Metin, "Anionic dye removal from aqueous solutions using modified zeolite: Adsorption kinetics and isotherm studies," *Chemical Engineering Journal*, vol. 200, pp. 59–67, 2012. https://doi.org/10.1016/j.cej.2012.06.038

[3] H.A. Awala and M.M. El Jamal, "Equilibrium and kinetics study of adsorption of some dyes onto feldspar," *Journal of the University of Chemical Technology and Metallurgy*, vol. 46, no. 1, pp. 45-52, 2011.

[4] S. Bhattacharjee, "Adsorptive removal of methylene blue using *Azadirachta indica* (neem) leaf," *International Research Journal of Environment Sciences*, vol. 5, no. 1, pp. 21-24, 2016.

[5] S.P. Buthelezi, A.O. Olaniran, B. Pillay, "Textile dye removal from wastewater effluents using bioflocculants produced by indigenous bacterial isolates," *Molecules*, vol. 17, pp. 14260–14274, 2012. https://doi.org/10.3390/molecules171214260

[6] G. Crini, "Non-conventional low-cost adsorbents for dye removal: a review," *Bioresource and Technology*, 97, 1061-1085, 2006. https://doi.org/10.1016/j.biortech.2005.05.001

[7] Das, S. and Barman, S., "Studies on removal of Safranine-T and methyl orange dyes from aqueous solution using NaX zeolite synthesized from fly ash," *International Journal of Science*, vol. 2, no. 4, pp. 735–747, 2013.

[8] Y. Deepti, "Equilibrium isotherm, kinetic and thermodynamic study on removal of methylene blue dye from aqueous solution by using corn cob activated carbon," *International Journal of Research in Chemistry and Environment*, vol. 6 no. 3, pp. 7-14, 2016.

[9] I.M. Eldien, A.A. Al-Sarawy, M.M. El-Halwany and F.R. El-Msaly, "Kinetics and Thermodynamics Evaluation of Activated Carbon Derived from Peanuts Shell as a Sorbent Material," *Chemical Engineering and uoJ Process Technology*, vol. 7, no. 267, 2016. doi:10.4172/2157-7048.1000267.

[10] M.F. Elkady, M.R. El-Aassar and H.S. Hassan, "Adsorption profile of basic dye onto novel fabricated carboxylated functionalized co-polymer nanofibers," *Polymers*, vol. 8, no. 177, pp. 1-13, 2016. doi:10.3390/polym8050177. https://doi.org/10.3390/polym8050177

[11] F. Gönen and F. Önalan, "Adsorptive removal behaviour of Procion MX-R dye from SRDW by chitosan," *Applied Ecology and Environmental Research*, vol. 14, no. 1, pp. 77-98, 2016. DOI: http://dx.doi.org/10.15666/aeer/1401_077098.

[12] R.H. Gumus, "Kinetic Studies of Methylene Blue Adsorption on to Activated Carbon Prepared from Plantain Pod (Musa paradisiac)," *British Journal of Applied Science and Technology*, vol. 15, no.3, pp. 1-14, 2016. https://doi.org/10.9734/BJAST/2016/24079

[13] V.K. Gupta and Suhas, "Application of low-cost adsorbents for dye removal: a review," *Journal of Environmental Management*, vol. 90, pp. 2313-2342, 2009. https://doi.org/10.1016/j.jenvman.2008.11.017

[14] R. Hariharasuthan, A.N. Rao and A. Bhaskaran, "Adsorption studies on reactive blue 4 by varying the concentration of MgO in Sorel's cement," *Adsorption*, vol. 2, pp. 287–292, 2013.

[15] C.A. Igwegbe, P.C. Onyechi, O.D. Onukwuli and I.C. Nwokedi, "Adsorptive Treatment of Textile Wastewater Using Activated Carbon Produced from Mucuna pruriens Seed Shells," *World Journal of Engineering and Technology*, vol. 4, pp. 21-37, 2016. https://doi.org/10.4236/wjet.2016.41003

[16] N.T. Joseph, O.E. Chinonye, I.K. Philomena, A.C. Christian and O.C. Elijah, "Isotherm and kinetic modeling of adsorption of dyestuffs onto kola nut (*Cola acuminata*) shell activated carbon," *Journal of Chemical Technology and Metallurgy*, vol. 51, no. 2, pp. 188-201, 2016.

[17] M.I. Khan, M.A. Khan, S. Zafar and S.A. Hussain, "Adsorption kinetics and thermodynamics study for the removal of anionic dye Eosin-B from aqueous solution by anion exchange membrane: adsorption kinetics and thermodynamics," *Scholars Journal of Engineering and Technology (SJET)*, vol. 3, no.9, pp. 741-749, 2015.

[18] M.R.R. Kooh, M.K. Dahri and L.B.L. Lim, "The removal of rhodamine B dye from aqueous solution using Casuarina equisetifolia needles as adsorbent," *Cogent Environmental Science*, vol. 2, 1140553, 2016. http://dx.doi.org/10.1080/23311843.2016.1140553

[19] B. Meroufel, O. Benali, M. Benyahia, Y. Benmoussa and M.A. Zenasni "Adsorptive removal of anionic dye from aqueous solutions by Algerian kaolin: Characteristics, isotherm, kinetic and thermodynamic studies," *Journal of Material and Environmental Science*, vol. 4, no. 3, pp. 482-491, 2013.

[20] Y. Miyah, A. Lahrichib, M. Idrissi, "Removal of cationic dye – methylene blue – from aqueous solution by adsorption onto corn cob powder calcined," *Journal of Material and Environmental Science*, vo. 7, no. 1, pp. 96-104, 2016.

[21] V.R. Parate and M.I. Talib, "Utilization of pulse processing waste (*Cajanus cajan* husk) for developing metal adsorbent: a value-added exploitation of food industry waste," *American Journal of Food Science and Technology*, vol. 3, no. 1, 1-9, 2015. DOI:10.12691/ajfst-3-1-1

[22] T.K. Saha, N.C. Bhoumik, S. Karmaker, M.G. Ahmed, H. Hideki Ichikawa and Y. Fukumori, "Adsorption of methyl orange onto chitosan from aqueous solution," *Journal of Water Resource and Protection*, 2, 898-906, 2010. doi:10.4236/jwarp.2010.210107

[23] T.A. Salman and M.I. Ali, "Potential application of natural and modified orange peel as an eco–friendly adsorbent for methylene blue dye," *Iraqi Journal of Science*, 2016, vol. 57, no. 1A, pp. 1 -13, 2016.

[24] M.R., Samarghandi, M., Hadi, S. Moayedi, and F.B. Askari, "Two-parameter isotherms of methyl orange sorption by pinecone derived activated carbon," *Iranica Journal of Environmental Health, Science and Engineering*, vol. 6, no. *4*, pp. 285-294, 2009.

[25] R. Srivastava and D.C. Rupainwar, "A comparative evaluation for adsorption of dye on neem bark and mango bark powder," *Indian Journal of Chemical Technology*, vol. 18, pp. 67-75, 2011.

[26] D.R. Tchuifon, S.G. Anagho, E. Njanja, J.N. Ghogomu, N.G. Ndifor-Angwafor and T. Kamgaing, "Equilibrium and kinetic modelling of methyl orange adsorption from aqueous solution using rice husk and egussi peeling," *International Journal of Chemical Science*, vol. 12, no. 3, pp. 741-761, 2014.

[27] Y.-H. Shih, C.-P. Tso and, L.-Y. Tung, "Rapid degradation of methyl orange with nanoscale zerovalent iron particles," *Journal of Environmental Engineering and Management*, vol. 20, no. 3, pp. 137-143, 2010.